



ELSEVIER

Available online at www.sciencedirect.com

SCIENCE @ DIRECT®

Earth and Planetary Science Letters 232 (2005) 109–123

EPSL

www.elsevier.com/locate/epsl

The detection of bacterial magnetite in recent sediments of Lake Chiemsee (southern Germany)

Yongxin Pan^{a,b,*}, Nikolai Petersen^{b,1}, Alfonso F. Davila^{b,2}, Liming Zhang^{b,3}, Michael Winklhofer^{b,4}, Qingsong Liu^{a,c,5,6}, Marianne Hanzlik^{d,7}, Rixiang Zhu^{a,8}

^aState Key Lab of LTE, Institute of Geology and Geophysics, Chinese Academy of Sciences, Beijing 100029, PR China

^bDepartment of Earth and Environmental Science, Ludwig-Maximilians-University, Munich 80333, Germany

^cInstitute for Rock Magnetism, University of Minnesota, Minneapolis, MN 55455, USA

^dDepartment of Chemistry, Technical University of Munich, D-85748 Garching, Germany

Received 17 September 2004; received in revised form 3 January 2005; accepted 7 January 2005

Editor: V. Courtillot

Abstract

The sediments of Lake Chiemsee, located in the Alpine foreland in Southern Germany, host a variety of magnetotactic bacteria (MTB), which contain intracellular crystals of magnetite arranged in linear chains. To detect bacterial magnetite in the carbonate-dominated surface sediments and further quantify its contribution to the magnetic signal of the sediments, we conducted detailed rock magnetic measurements as well as complimentary non-magnetic analyses (electron microscopy, powder X-ray diffraction, and sediment pore-water analysis). Our results demonstrate that biogenic single-domain magnetite (characterized by bullet- and truncated hexagonal prismatic shapes) is the dominant ferrimagnetic component in the topmost few centimetres of the sediment. The changes of magnetic properties with depth are due to the occurrence of live MTB and the downward increasing dissolution of biogenic magnetite. Moreover, the ratios of remanence loss on warming through the Verwey transition after field cooling and zero-field cooling of saturation isothermal remanence (δ_{FC}/δ_{ZFC}) were determined as 1.47 and 1.25 for freeze-dried and air-dried sediment samples containing MTB, respectively. These low ratios suggest that the bacterial magnetite chains were disrupted to a large extent and/or that the bacterial magnetosomes might have undergone partial

* Corresponding author. Tel.: +86 10 6200 7913; fax: +86 10 6201 0846.

E-mail addresses: yxpan@mail.iggcas.ac.cn (Y. Pan), petersen@geophysik.uni-muenchen.de (N. Petersen), fon@geophysik.uni-muenchen.de (A.F. Davila), liming.zhang@lrz.uni-muenchen.de (L. Zhang), michael@geophysik.uni-muenchen.de (M. Winklhofer), liux0272@yahoo.com (Q. Liu), marianne.hanzlik@ch.tum.de (M. Hanzlik), rxzhu@mail.iggcas.ac.cn (R. Zhu).

¹ Tel.: +49 89 21804233.

² Tel.: +49 89 21804326.

³ Tel.: +49 89 21804356.

⁴ Tel.: +49 89 21804207.

⁵ Present address: Department of Earth Sciences, University of California at Santa Cruz, Santa Cruz, CA 95064, USA.

⁶ Tel.: +1 831 459 4847.

⁷ Tel.: +49 89 28913235.

⁸ Tel.: +86 10 62007912.

0012-821X/\$ - see front matter © 2005 Elsevier B.V. All rights reserved.

doi:10.1016/j.epsl.2005.01.006

low-temperature oxidation. It is proposed that although rock magnetic measurements are suitable for quantifying the contribution of fine-grained particles to the overall magnetic signal of sediments, complementary non-magnetic methods are essential to unambiguously identify its bacterial origin.

© 2005 Elsevier B.V. All rights reserved.

Keywords: rock magnetism; biogenic magnetite; delta ratio; remanence coercivity spectrum; Lake Chiemsee

1. Introduction

Intracellular magnetite crystals (magnetosomes) in cells of magnetotactic bacteria (MTB) usually have distinct species-specific crystal morphology, a narrow grain-size distribution and are arranged in the form of single or multiple chains. Bacterial magnetite has been found in many sedimentary environments from anoxic deep-sea sediments to oxic soils since the first discovery of MTB three decades ago [1–6]. Ranging dominantly within the stable single-domain (SD) region, fossil magnetosomes often leave a stable imprint on the paleomagnetic signature of sediments (e.g. [7–9]). The biological activity in sediments and the production of bacterial magnetite depend on environmental changes and therefore variations in biogenic magnetite contents can be used for reconstructing past climatic changes [10–14]. However, biogenic magnetite is also prone to be dissolved under reducing conditions due to its small particle size (e.g. [15]). The input of organic matter must therefore be low, or at least, be fully consumed at the sediment surface in order for bacterial magnetite to survive over geological time scales and so contribute to the paleomagnetic or -environmental records. Carbonate-rich sediments with moderate accumulation rate and weakly oxic or sub-oxic chemistry may provide the most favourable conditions for the preservation of fossil magnetosomes of magnetite.

The surface calcareous sediments of the Alpine foreland Lake Chiemsee (southern Germany) have long been documented to host plenty of live MTB [16]. Among several species of MTB described in Lake Chiemsee sediments, the so-called *Magneto-bacterium bavaricum* is particularly interesting as it contains up to a thousand bullet-shaped magnetite crystals, which are arranged in 2–5 linear chains [17]. Owing to their characteristic crystal shape, magneto-

somes of *M. bavaricum* can easily be recognized as such in magnetic extracts from sediments using a transmission electron microscope (TEM). In order to evaluate the contribution of bacterial magnetite to the bulk magnetic properties of the lake surface sediments, we conducted a combined investigation using rock magnetic techniques in conjunction with a set of non-magnetic approaches such as transmission and scanning electron microscopy (TEM and SEM) and powder X-ray diffraction (PXRD). Our second aim is to test the fidelity of rock-magnetic diagnostic criteria for identifying biogenic magnetite in bulk sediments. After studying the magnetic properties of cultured MTB, Moskowitz et al. [18] proposed a combination of room-temperature coercivity and low-temperature remanence warming measurements to detect the presence of intact chains of bacterial SD magnetite in sediments. Whether rock magnetic criteria derived from measurements on cultured MTB cells may hold for natural sediment samples however remains uncertain. This uncertainty arises from the fact that natural samples usually host more than one species of MTB, and from the unknown preservation state of the magnetosomes in the sediments.

2. Samples

Lake Chiemsee is located in the Alpine foreland, 80 km southeast of Munich (Fig. 1). It covers an area of 80 km² with a maximum water depth of 74 m. The small catchment is dominated by carbonate bedrock, giving rise to rather high pH (~8.3) in the lake. The water column is oxygen saturated down to the water/sediment interface [19]. A variety of different forms of live MTB, mainly rod-shaped *M. bavaricum*, wildtype cocci and spirilli, were found in the upper few centimetres (~2 cm) of the sediments with a maximum

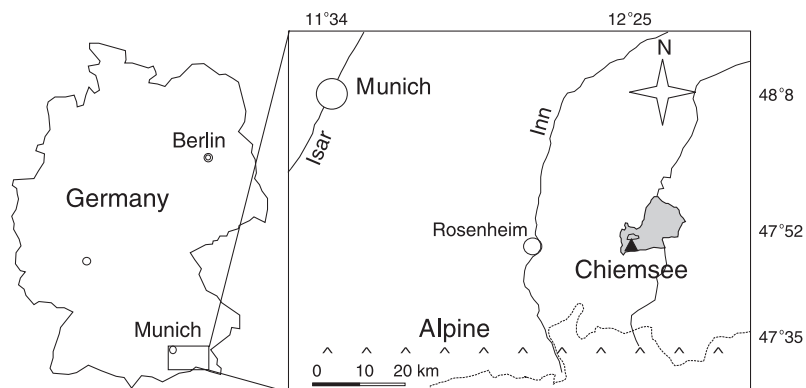


Fig. 1. The location of Lake Chiemsee and sampling sites of this study (triangle).

population density as high as approximately 10^7 /ml. Previous TEM analyses [17,20] revealed that the bacterial magnetosomes of *M. bavaricum* and cocci consisted solely of magnetite.

Four piston cores (~25 cm in length and labelled “CO-01...CO-04”) were collected in July and October 2003, respectively, using a laboratory-made piston core device, at a water depth of approximately 20 m, where a high population density of live MTB had been reported previously. For comparison, a piston core in a different site at a water depth of 40 m (labelled “KO-01”) was also collected. Here the sediments contain more organic matter and therefore are under more reducing conditions, compared to the 20 m cores. The short cores were kept vertical after collection although some mixing between the sediment/water interface might have occurred during transportation. The samples were kept in a refrigerator to prevent possible alteration during laboratory storage. Every piston core was re-sampled in the laboratory at 1 cm intervals for high-resolution magnetic measurements.

In addition to the piston cores, surface bulk sediment samples from the area of 20 m water depth were collected using a scratching device. The material approximately corresponds to the upper 5 cm of the piston cores. The scratched samples were then placed in 120 cm³ aquariums. Examination of the newly collected sediment samples under a light microscope in a controlled magnetic field (referred to as Bacteriodrome [16]) confirmed the presence of live MTB in great numbers, with *M. bavaricum* and wild-type cocci as predominant species in the samples from 20

m water-depth. Samples of pure MTB were obtained from these sediments by “step-by-step” collection under the microscope. Only a few magnetic cocci were found in the samples from 40 m water-depth. Furthermore, our PXRD analyses demonstrated that sediments are dominated by calcite, along with some quartz and a small amount of siderite.

3. Methods

3.1. Magnetic measurements

Room temperature and high temperature rock magnetic measurements were conducted on 145 bulk sediment samples from three piston cores (CO-01, 02 and 03) and the scratched surface sediments to characterize the magnetic mineral phases, their concentration and grain sizes. Low-field magnetic susceptibility was measured using a Bartington MS2 susceptibility meter. Measurements of isothermal remanent magnetization (IRM) acquisition, back-field demagnetization of saturation IRM (SIRM) and hysteresis loops were conducted on a variable-field translation balance (VFTB), which allows the measurement of samples of up to 0.5 g in weight in a maximum applied field of 1 T.

Thermomagnetic curves (J – T) up to 700 °C were measured on all samples using the VFTB device to determine the Curie point of magnetic minerals and monitor thermal alterations. Samples were heated at a rate of 10 °C/min in air in an applied field between 15 and 430 mT.

The remanence coercivity spectra analyses on representative samples are used here to distinguish between high-coercivity and low-coercivity phases. Stepwise SIRM acquisition, static field and alternating field (AF) demagnetizations were conducted on representative bulk sediment samples. For comparison, samples from 20 m water-depth (named MTB-rich) and samples from 40 m water-depth (named MTB-poor) were measured. The MTB in the samples were examined using the Bacteriodrome, prior to the measurements. All remanence measurements were made along a single axis. Remanence was measured using a 2G cryogenic magnetometer.

Anhyseretic remanent magnetization (ARM) acquisition and AF demagnetization were also performed on sister samples. A remanence was imparted stepwise in an AF fields of increasing peak values from 5 to 150 mT with a steady bias DC field (0.05 mT) and was measured by a 2G cryogenic magnetometer, followed by stepwise AF demagnetization using a 2G degausser.

We measured the loss of SIRM during warming in zero-field after samples were cooled both in zero-field (ZFC) and in a strong field of 5 T (FC) using a Quantum Design Magnetic Property Measurement System (MPMS-XL) at the University of Bremen. The remanence after exposure to 5 T at 5 K was measured at intervals of 2–5 K during warming in zero field from 5 to 300 K after cooling from 300 K. The remanent field in the cavity was less than 0.2 mT.

3.2. Non-magnetic measurements

To characterize further the magnetic components in the surface bulk sediments, PXRD and electron microscopic examinations were conducted on magnetic extracts. Magnetic extracts were obtained from sediments in both piston cores and aquariums using a high magnetic gradient. Before magnetic extraction, sediments were stirred using distilled water and were ultrasonically dispersed. To remove non-magnetic components in the magnetic extracts, the extraction procedure was applied iteratively to the extracts two or three times. PXRD was performed using a computer-controlled STOE STDIP focusing diffractometer equipped with a curved Ge (111) monochromator, where Mo K α radiation was used ($\lambda_{\text{Mo}}=0.07093$ nm) in the angular range $4^\circ < 2\theta < 54^\circ$. The

resulting minimum half width (FWHM) was 0.10° and a step width of $\delta(2\theta)=0.02^\circ$ was applied. The crystal structure was determined using routines for indexing DICVOL and for Rietveld refinement FULLPROF. Due to insufficient samples, no internal standard was used.

Electron microscopic examinations using a JEOL JSM5900 SEM and a JEOL JEM100CX TEM were conducted at the Technical University of Munich to check whether the surface bulk sediment samples contain bacterial magnetite (fossil magnetosomes). For TEM observation, the unconsolidated sediment samples were stirred in a small volume of distilled water and thoroughly dispersed by high power ultrasonics. The magnetic particles were extracted with a magnetic finger as described by [2]. A drop of the extracted material was then let dry off on a TEM grid.

We also measured geochemical profiles of the fresh sediment pore water on the piston core (CO-04) to monitor chemical variations. The piston core was cut into 1.5 cm thick slices, which were centrifuged to extract sufficient pore water. The concentrations of nitrate and sulphate of the pore water were measured by an ICS Ion Chromatography System.

4. Results

4.1. Low field magnetic susceptibility, hysteresis and thermomagnetic measurements

The carbonaceous sediments show low magnetic susceptibilities, ranging from 2.3 to 7.4×10^{-5} SI, with a mean value of 5.9×10^{-5} SI for samples from 20 m water-depth. The average susceptibility is 5.4×10^{-5} SI for samples from 40 m water-depth. Our samples were too weak for the susceptibility meter to measure reliable frequency dependent susceptibilities.

Room temperature remanence and hysteresis measurements yielded coercive force (B_c) and remanent coercivity (B_{cr}) values of 11.1–22.3 mT and 34.2–52.9 mT, with a mean value of 17.9 ± 3.1 mT and 45.7 ± 3.3 mT, respectively. SIRMs (or SIRM values) are in the range of $0.2\text{--}3.2 \times 10^{-6}$ Am 2 kg $^{-1}$. Hysteresis loops of the surface sediment are slightly pot-bellied (Fig. 2). Both SIRM acquisition and hysteresis loops show a saturation field generally lower than 200–300 mT.

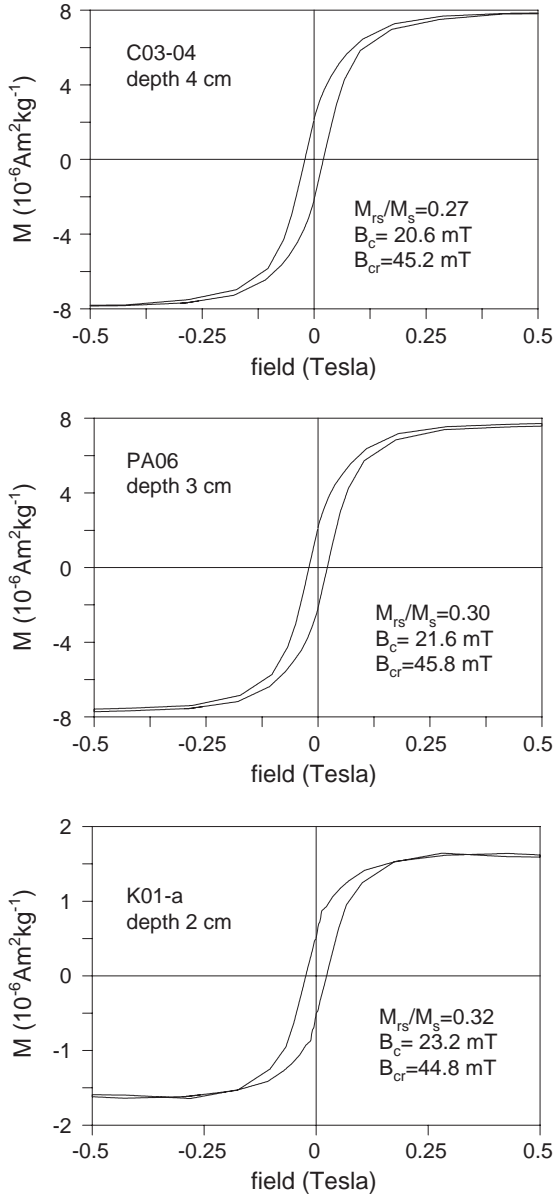


Fig. 2. Typical hysteresis loops of surface bulk sediments. The maximum applied field is 1 T (not shown). B_c , B_{cr} , M_{rs} , and M_s refer to coercive force, coercivity of remanence, saturation remanence, and saturation magnetization, respectively.

Ratios of saturation remanence to saturation magnetization (M_{rs}/M_s) and coercivity of remanence to coercive force (B_{cr}/B_c) range between 0.15–0.32 and 1.9–4.6, respectively. As seen in Fig. 3, the sediments from the upper interval (<5 cm) on average

have higher M_{rs}/M_s (0.28 vs. 0.22) and lower B_{cr}/B_c (2.50 vs. 3.36) ratios than sediments from the greater depth (≥ 5 cm), pointing to a higher concentration of fine-grained material in the upper sediment interval. This is in agreement with our observation that live MTB were most abundant in the upper few centimetres of the sediments. Samples from 40 m water depth generally have rock magnetic properties similar to the 20 m water-depth samples, but lower SIRMs and susceptibilities, suggesting lower concentration of magnetic particles.

A typical J – T curve is presented in Fig. 4, showing distinct alteration upon heating above 440 °C, which blurs the signal of the primary phase. To determine the

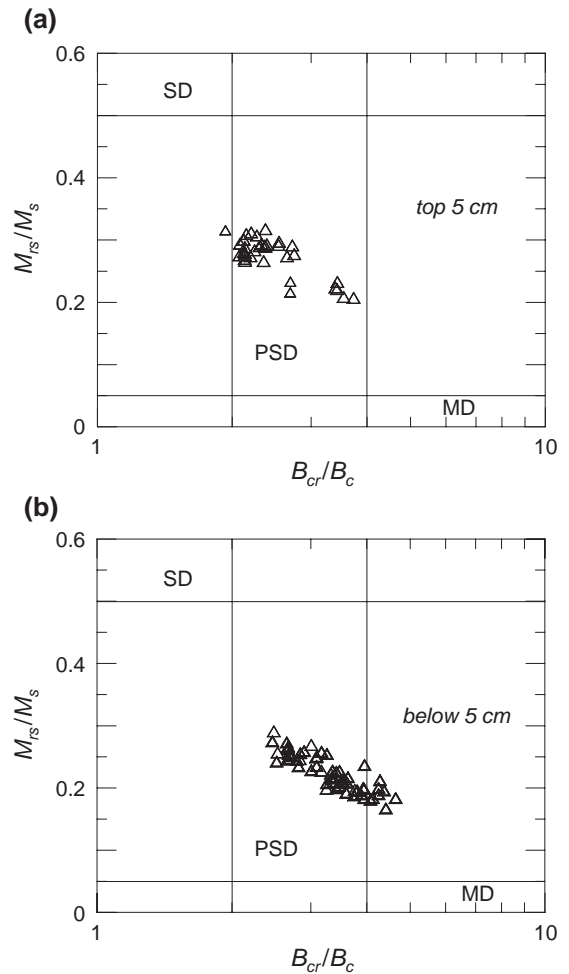


Fig. 3. Day-plots of upper surface sediments (<5 cm) (a) and sediments from greater depth (>5 cm) (b).

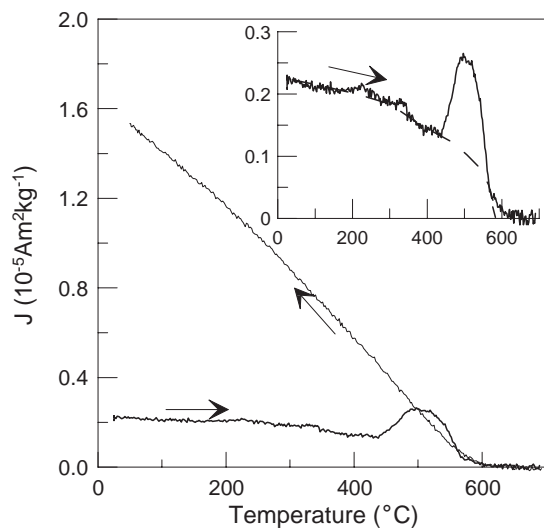


Fig. 4. Representative thermomagnetic curve of a bulk sediment sample (heating in air, field strength: 35.8 mT). The dashed line in the inset shows an eye-estimate component of magnetite, which is blurred by transformation of new magnetic phases by heating.

Curie point (T_C) of the dominant magnetic phase before alteration, we fitted the <440 °C part of the J – T curve with a $((T_C - T)/(T_C - T_0))^{0.43}$ law (where T_0 is the room temperature) and obtained 570–580 °C as the Curie point by extrapolating (inset in Fig. 4), indicative of magnetite ($T_C=580$ °C) as the main primary ferromagnetic constituent. A significant increase occurs between 450 and 510 °C, followed by a rapid drop to nearly zero around 600 °C. This significant change seen in all measured samples could be a result of the transformation of the paramagnetic siderite into magnetite and/or maghemite and/or oxidation of iron sulphides. Besides this pronounced alteration feature, there is a small increase around 200–250 °C followed by small hump of magnetization around 320 °C, probably due to thermal formation of a new phase (e.g. pyrrhotite).

4.2. Acquisition and demagnetization analyses of SIRM

Typical remanent coercivity spectra of MTB-rich and MTB-poor samples are presented in Fig. 5, and compared with data of a pure MTB sample (Pan et al., unpublished data). The median remanent coercivities of the MTB-rich, MTB-poor and the pure MTB

samples are 48 mT, 43 mT and 50 mT, respectively. The demagnetization curve of both MTB-rich and MTB-poor samples decay faster than the MTB sample and have median destructive field (MDF) values between 30 and 35 mT, $\sim 2/3$ of the MTB sample. The intersection (R -value) of SIRM acquisition and AF demagnetization is distinctly less than 0.5, suggesting magnetic interaction of magnetic particles in the bulk sediment samples [21].

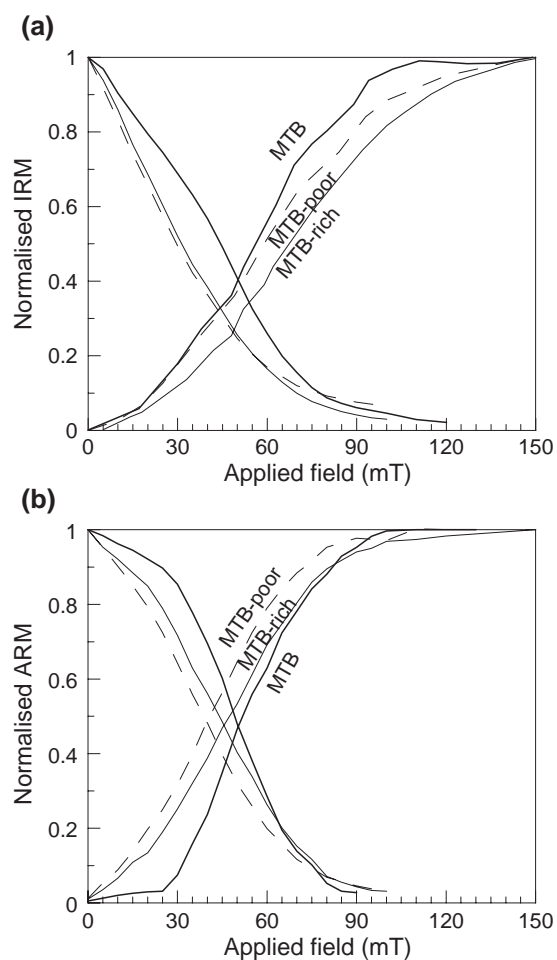


Fig. 5. Comparison of representative remanent coercivity spectra analyses of bulk sediment samples. Sample 20-2 from 20 m water-depth (MTB-rich, solid line), sample 40-4 from 40 m water-depth (MTB-poor, dashed line) and pure MTB sample (coarse line). (a) SIRM acquisition and AF demagnetization. (b) ARM acquisition and AF demagnetization.

4.3. Anhyseretic remanent magnetization (ARM)

Fig. 5b shows a comparison of ARM acquisition and demagnetization of the pure MTB sample (Pan et al., unpublished data), the MTB-rich and the MTB-poor sediment samples. The median remanent coercivities are 51 mT, 46 mT, and 40 mT, respectively. A distinct feature is that both the coercivity of the MTB-rich sample and its curve lie between the other two. The R -values of the samples are close to 0.5.

Moreover, the significant positive difference of the MDFs of ARM and IRM, i.e. ($MDF_a - MDF_i$), for both MTB-rich and MTB-poor samples are also indicative of very fine-grained SD magnetite in the sediments [22].

4.4. Low temperature SIRM demagnetization

Two fresh bulk aquarium sediment samples containing plenty of live MTB were selected for the measurements. One sample was freeze-dried and the other was air-dried before the measurements. Both ZFC and FC warming curves show a drop of remanence below 30–40 K (not shown), which may relate to a superparamagnetic component and/or siderite in the samples. A distinct remanence drop around 100–115 K (see Fig. 6) indicates the Verwey transition of magnetite (~120 K), but shifted to a lower temperature. Interestingly, the two samples have a different Verwey transition temperature (T_v), here defined as the temperature at which the derivative dM/dT is at maximum. Compared to T_v of the freeze-dried sample (Fig. 6a), T_v of the air-dried sample (Fig. 6b) is further shifted to lower temperatures, suggesting some extent of oxidation. Above 130 K, the remanence decreases gradually with temperature.

The delta ratio (δ_{FC}/δ_{ZFC}) was calculated according to the definition by Moskowitz et al. [18], $\delta = (M_{80K} - M_{150K})/M_{80K}$, and obtained as 1.47 and 1.25 for the freeze-dried and air-dried samples, respectively. Both values are greater than 1.2, which according to [18] is the upper value for the purely inorganic end member, but lower than the minimum value of 2 for the end member representing solely magnetite arranged in chains. Our δ -ratios are also slightly lower than the threshold (1.5) for a positive chain response in mixtures of chains and inorganic magnetite (see case 3 in [18]).

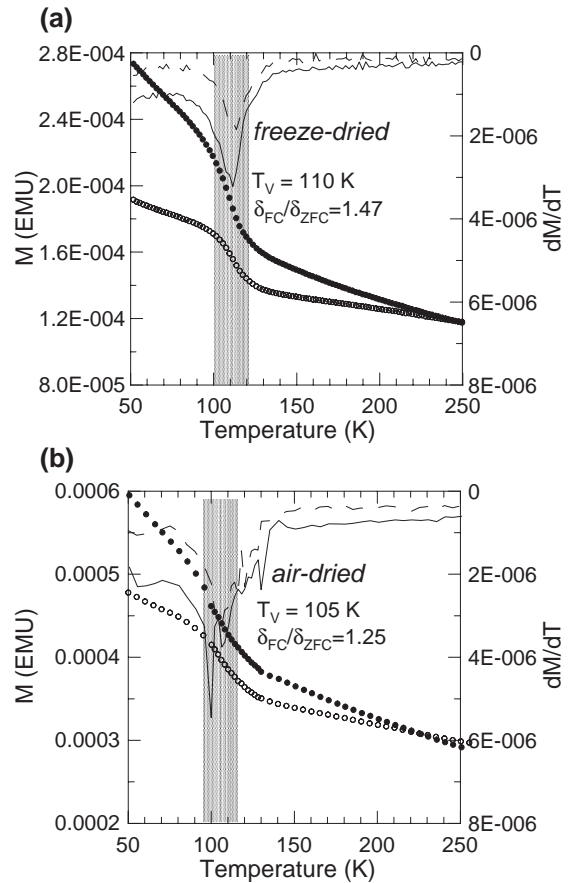


Fig. 6. Low-temperature saturation remanence demagnetization curves after samples were cooled in field cooled (FC, solid circles) and in zero-field cooled (ZFC, open circles) of freeze-dried and air-dried bulk sediments containing MTB. δ is defined as $(M_{80K} - M_{150K})/M_{80K}$ [18]. Solid (dashed) lines refer to the first derivative, dM/dT , of warming curve after FC (ZFC) cooling, respectively. T_v is the temperature of the Verwey transition, here defined as the temperature at which dM/dT is maximum (grey shading).

4.5. Powder X-ray diffraction (PXRD)

Fig. 7 presents typical PXRD results of magnetic extract samples from a piston core collected from 20 m water-depth. It shows that magnetite is the dominant phase. This further confirms the results obtained from rock-magnetic measurements on bulk sediment samples. In addition, along with detrital quartz, small amounts of maghemite and iron sulphide (greigite) were detected in magnetic extracts from sediments above and below 5 cm, respectively.

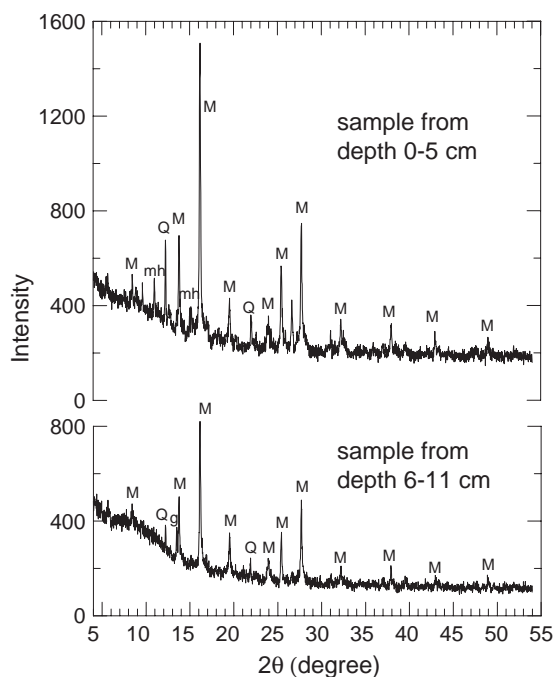


Fig. 7. Powder X-ray diffraction (PXRD) results of magnetic extract samples from a piston core collected from 20 m water-depth. M, mh, Q, and g refer to magnetite, maghemite, quartz and greigite, respectively. Mo K α radiation was used.

4.6. Electron microscopic examinations

Electron microscopic observations on magnetic extracts showed fine-grained bacterial magnetite in coexistence with coarser-grained detrital magnetite crystals. Iron oxyhydroxide and industrial iron spherules were found, too. Fig. 8a–c shows magnetosomes from the surface-sediment samples studied. An intact cell of *M. bavaricum* with hundreds of magnetite magnetosomes was observed (Fig. 8a). The originally linear chains of magnetosomes were disrupted, probably as a consequence of cell shrinkage during dehydration [23]. These magnetite magnetosomes are bullet-shaped (Fig. 8b), with typical dimensions of 35 nm and 120 nm for the short and long axis, respectively, and fall well in the stable single domain (SSD) magnetite range [24]. Prismatic-shaped and truncated hexagonal prismatic magnetite crystals arranged in a disfigured chain (Fig. 8c) resemble magnetosomes observed in cocci or spirilla [20]. Fig. 8d–f show needle-shaped iron oxyhydroxide crystals, anthropogenic iron spherules,

and coarse-grained detrital magnetite with rounded corners, respectively.

4.7. Downcore variations of rock magnetic properties and sediment pore-water geochemistry

Rock magnetic measurements were carried out on piston cores (~25 cm) collected at 20 m water-depth to check variations of magnetic properties with depth. All three measured cores showed similar downcore patterns (Fig. 9a–g). The most distinct boundary was observed at ~5 cm. All measured rock magnetic parameters below this depth remain relatively stable. In contrast, for samples between 2 and 5 cm, B_c , SIRM, and M_s increase steadily upward. The inter-parametric ratios (sensitive to grain size variations) $SIRM/\chi$ and M_{rs}/M_s show the same trend. For the topmost samples (<2 cm), an opposite trend is observed for SIRM (Fig. 9c), but the grain size parameters B_{cr}/B_c (Fig. 9f) and M_{rs}/M_s (Fig. 9g) remain relatively stable.

Fig. 9h shows the downcore variation of the pore-water geochemical parameters. It is noted that nitrate content increases downward to ~5 cm (reaching a maximum of 0.799 mg/l), then decreases to 13 cm and are of undetectable level below. The sulphate concentration (maximum 10.46 mg/l) first decreases with depth, reaches a minimum at around 10 cm and then increases again, with values at depths below 18 cm similar to those in the top few cm (Fig. 9h). We note that the peaks in the downcore plots of SIRM and $SIRM/\chi$ correspond to the relatively high levels of nutrients.

Based on rock-magnetic properties and pore-water geochemistry, the upper 25 cm surface sediments can be divided into four zones (Fig. 9): I, <~2 cm; II, ~2–5 cm; III, 5–15 cm; and IV, >15 cm.

5. Discussion

5.1. Origin of magnetic minerals in lake sediments

To quantitatively decipher the rock magnetic properties of lake sediments in terms of environment and ecology, it is necessary to identify the origin of the magnetic minerals. Four possible genetic categories are: (1) detrital input, (2) anthropogenic pollu-

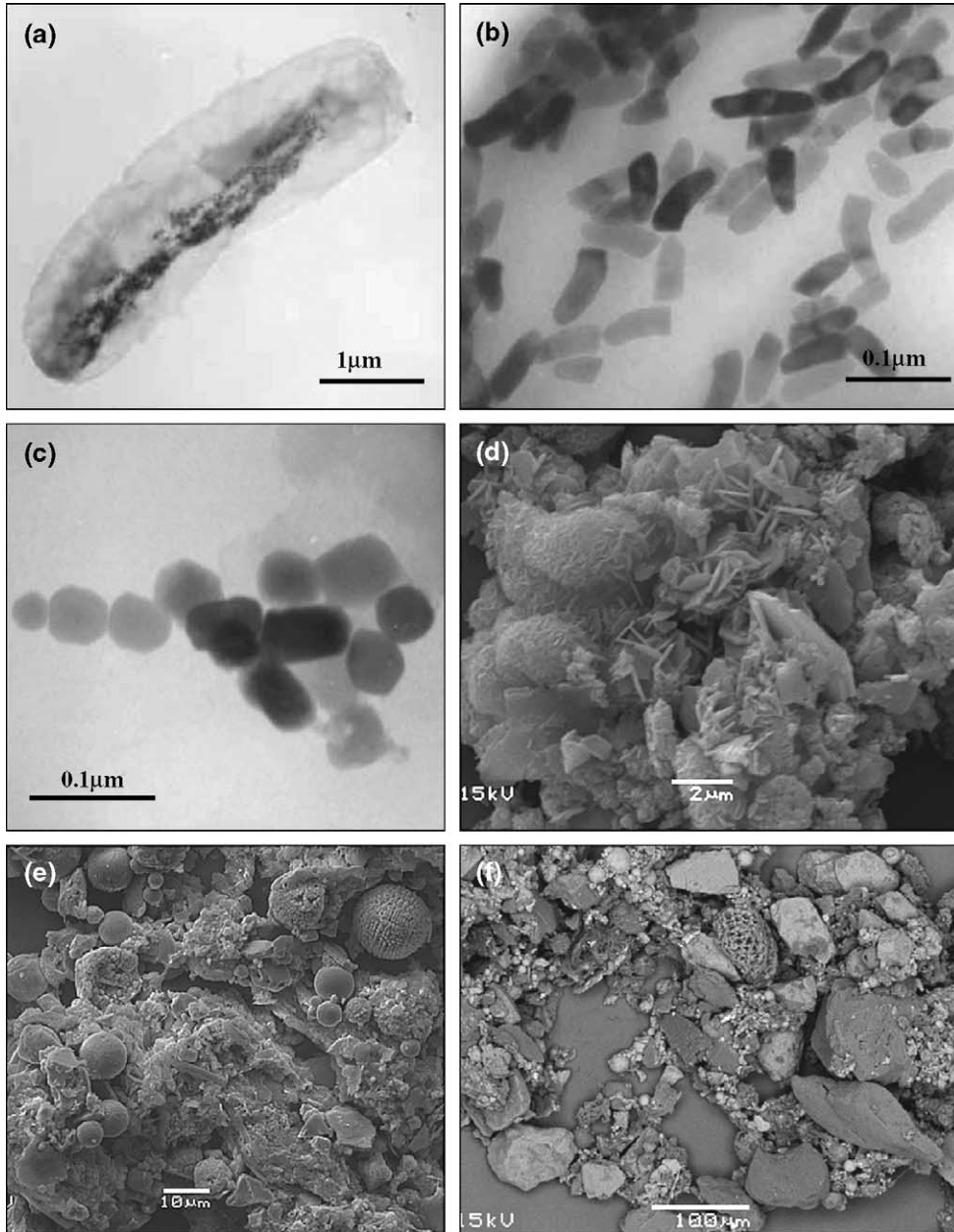


Fig. 8. Micrographs of electron microscope observations on magnetic extracts from Lake Chiemsee. (a) A whole fossil cell of *M. bavaricum* and magnetosomes; (b) bullet-shaped magnetosomes of *M. bavaricum*; (c) prismatic shape magnetosomes (from cocci or spirilla) in short chain; (d) needle-like iron oxyhydroxide grains; (e) iron spherules from industrial pollution; (f) detrital coarse-grained magnetite particles.

tants, (3) authigenic phases formed by in situ precipitation or transformation of existing phases as a consequence of changes in pore-water chemistry brought about by inorganic processes and microbial

activities, and (4) biologically controlled mineralization products.

The surface sediments of Lake Chiemsee contain coarse-grained (>1 μm) iron spherules and angular

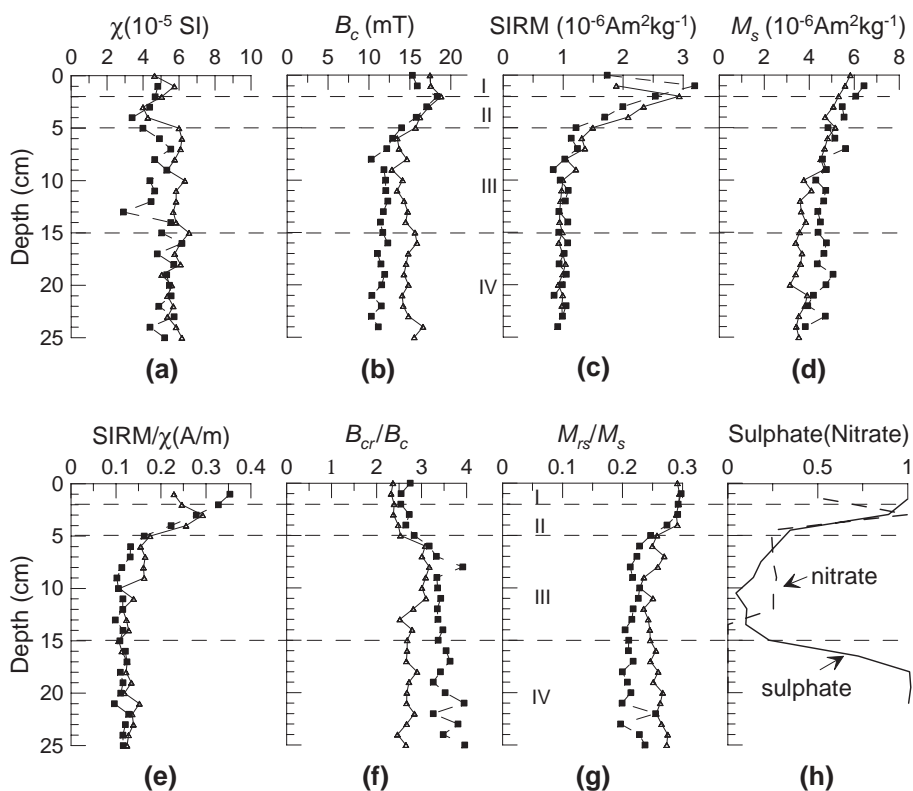


Fig. 9. Variations of magnetic parameters in piston cores (squares, CO-02; triangles, CO-03) (a to g) and comparison with chemical changes in sediment pore-water of CO-04 (g) as a function of depth. χ is low field magnetic susceptibility, SIRM, the saturation remanence. Both sulphate and nitrate contents were normalised to their corresponding maximum values.

magnetite particles with rounded corners (Fig. 8e,f). The spherules reflect local pollution from power plants or vehicle emissions, while the angular magnetite crystals are erosion products. Because of the small catchment, nearby bedrocks or sediments are the prevailing sources of the detrital input.

Siderite and iron sulphides are most likely in situ precipitates in our calcareous sediments. In the zone where pore-water sulphate is low (Zone III), dissolved ferrous iron can react with hydrogen carbonate to yield siderite,



On the other hand, microbial mediated formation of siderite could not be ruled out [20]. At greater depths, the concentration of pore-water sulphate is 10 times

larger than in Zone III and the dissolved iron can react with sulphate to form iron sulphides.

The fourth category of magnetic phases consists of SD and fine-grained PSD magnetite particles, comprising dead cells of MTB and fossil magnetosomes (Fig. 8a–c). All fine-grained magnetite particles revealed by TEM observations closely resemble bacterial magnetosomes (characterised by narrow distributions of grain-size, distinct crystal shape and width–length ratio). The same particles were observed in live MTB collected and are often arranged in chains, strongly supporting the biogenic origin of the fine-grained magnetite particles in the sediments. Single-domain magnetite can be formed inorganically from thermal decomposition of siderite under CO_2 atmosphere [25,26], but this mechanism requires heating above 400 °C, and can be excluded for our case.

5.2. Variations in magnetic properties with depth and environmental implications

Thermomagnetic curves and PXRD analyses showed that magnetite is dominant in sediments over the whole core length. Therefore, changes in the rock magnetic parameters reflect variations in grain size and concentration of magnetite. These variations can be explained by the occurrence of live MTB in the topmost cm of the sediment and the downcore changes in the chemical environment, leading to progressive dissolution of the biogenic magnetite fraction, a phenomenon commonly observed in anoxic, reducing environments [27]. The apparent correlation between the geochemical parameters and the magnetic properties supports this hypothesis.

Similar to previous reports [28,29], our checks of the surface sediments using the Bacteriodrome showed that the topmost few centimetres of the sediment at the sampling sites host high numbers of live MTB, indicating the preferred habitat of MTB close to the sediment/water interface, i.e. Zones I and II in our case. Driven by changing redox conditions during the sediments accumulation process, live MTB tend to swim upward along the local geomagnetic line and enrich in the topmost few centimetres, leading to a significant increase in concentration of SD magnetite.

5.3. The delta ratio δ_{FC}/δ_{ZFC}

Moskowitz et al. [18] introduced the delta ratio as a diagnostic magnetic parameter for identification of magnetosome chains. The test is based on two facts, 1) that the monoclinic phase of magnetite at low temperature has a much stronger magneto-crystalline anisotropy than the cubic phase and 2) that magnetosome chains have a pronounced shape anisotropy. As a result of 1), the magnetization of an individual magnetosome will point into one of the monoclinic c -axes at $T < T_v$; as a consequence of 2), those c -axes that are nearest to the chain axis will be preferentially occupied. A strong magnetic field applied during cooling however will outweigh the anisotropy due to the chain such that those c -axes nearest to the field axis will be preferentially occupied [30]. If the field is switched off at $T < T_v$ after FC cooling, the magnetization will be blocked in a metastable thermoremanence state, which is energetically less favourable

than the ZFC induced remanence state. After cooling through the T_v the magneto-crystalline anisotropy tensor undergoes a symmetry change and the thermoremanence can be unblocked.

Samples consisting purely of MTB with intact chains of magnetite magnetosomes have delta ratios (δ_{FC}/δ_{ZFC}) > 2 [18]. The delta ratios of our sediment samples, with abundant MTB and fossil magnetosomes, however are less than 1.5 for both freeze-dried and air-dried samples (see Fig. 6). This might be caused by the following reasons.

Firstly, a disruption of magnetosome chains, as seen by the TEM observations (Fig. 8a) may reduce the ratio δ_{FC}/δ_{ZFC} , as demonstrated previously by Moskowitz et al. [19] on cultured MTB. So far it is unclear to what extent the linear magnetosome chains are preserved intact in lake or marine sediments. Most likely only a fraction of them will be preserved.

Secondly, the low-temperature oxidation of bacterial magnetite, and consequent non-stoichiometry can also lower the delta ratio because the Verwey transition is highly sensitive to the degree of oxidation [31]. Fully oxidized magnetite does not display a Verwey transition and we can expect identical ZFC and FC curves with the delta ratio approaching unity. This may be the case for three carbonate samples that contained magnetofossils by Weiss et al. [32] with delta ratios of only 0.9–1.2. However, for a slight degree of oxidation, Carter-Stiglitz et al. [33] proposed that the delta ratio could be enhanced > 2 because the Verwey transition of the ZFC curve is more affected by oxidation than that of the corresponding FC curve. Our sediment samples might have suffered low-temperature oxidation with a corresponding shift of the Verwey transition to lower temperatures (Fig. 6). PXRD analyses on the magnetic extracts showed a unit cell of 8.3937, corresponding to the upper limit for stoichiometric magnetite [34,35], where complete suppression of the Verwey transition is expected.

Thirdly, the mixture of detrital magnetite particles could reduce the delta ratios. Previous studies on inorganic magnetite of different grain sizes yielded delta values between 1.0 and 1.2 [18]. Generally, the mixture of magnetosome chains with inorganic magnetite, maghemite, hematite and greigite leads to a decrease of the delta ratios. An unambiguous identification of magnetosomes (delta ratio greater

than 1.5) requires that the chain fraction exceed 40–50% of the MD/PSD fraction and 75% of the SD fraction [18]. This means that the chain fraction in both of our MTB-containing samples is not exceeding 60%.

5.4. Magnetic susceptibility, coercive force and remanence coercivity spectra

Oldfield [36] suggested a combination of low-field, frequency dependant and anhysteretic susceptibilities to isolate a magnetosome response. We also tested this method by measuring the low-field susceptibility (χ) and anhysteretic susceptibility (χ_{ARM}) of the surface sediments (MTB-rich and MTB-poor samples) and loess samples. It has been found that the ratios of anhysteretic susceptibilities to low-field susceptibilities, χ_{ARM}/χ , of MTB-rich, MTB-poor and loess are ~ 30.5 , 24.2 and 6.8, respectively. This indicates that χ_{ARM}/χ is a good

indicator of the presence of SD magnetite in bulk samples.

The values of coercive force (B_c) of SD magnetite have a wide range between ~ 20 to ~ 60 mT. Stacey and Banerjee [37] showed that the lowest coercivity of SD magnetite is about 20 mT. Moskowitz et al. [38] reported that the coercivity of bacterial SD magnetite in magnetotactic bacteria is ~ 28 mT in *M. magnetotacticum* containing equi-dimensional magnetosomes but 40–50 mT in MV-1. Higher coercivity values (48–60 mT) were found for SD magnetite with high internal stress in glass–ceramic samples [39] and in natural volcanic glasses [40]. In contrast, for stress-free SD magnetite (e.g. hydrothermally grown and precipitated), its coercivity is generally slightly larger than 20 mT [41]. The shape of SD magnetite also strongly affects its coercivity. For example, Tauxe et al. [42] predicted coercivities of 28, 41, 69 mT for stress-free magnetite of q (aspect ratio)=1.3, 1.5, 2, respectively. However, for bacterial magnetite, where we can

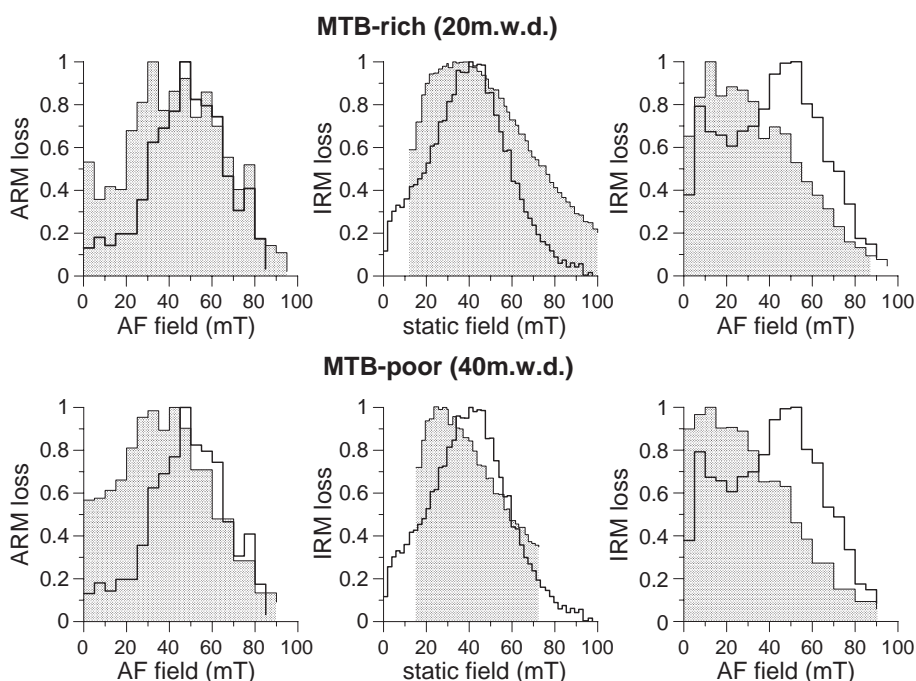


Fig. 10. Comparisons between remanence coercivity spectra analyses of representative MTB-rich sample (upper row) and MTB-poor sample (lower row) with pure MTB sample (coarse lines, unfilled). Remanence loss was normalised to the maximum value of the corresponding spectrum.

assume stress-free crystals, the relatively low coercivity ~ 20 mT indicates that the aspect ratio q is low.

Remanence coercivity spectra analyses of SIRM and ARM of the bulk sediments containing MTB showed median remanence coercivity values between 40 and 60 mT (Fig. 5). For theoretically non-interacting SD magnetite, the B_{cr} values estimated from these two methods should be identical. Measurement on whole cell samples of strain MV1-A by Moskowitz et al. [18] indicated a remanence coercivity of SIRM of ~ 50 mT. Chang et al. [43] also found that samples collected from carbonate oozes at Sugarloaf Key (Florida, USA) containing nearly pure bacterial single domain magnetite and living MTB had a remanence coercivity value of ~ 50 mT.

Fig. 10 shows further comparisons of remanence demagnetization spectra of the ARM and IRM between the pure MTB sample and the two type sediments of Lake Chiemsee, MTB-rich and MTB-poor. The spectra of the MTB-rich samples highly resemble that of the pure MTB sample, strongly supporting the hypothesis that biogenic SD magnetites are the main fine-grained component in the Lake Chiemsee surface sediments. Moreover, as seen from Figs. 5 and 10, our results suggest that remanent coercivity spectra of ARMs and IRMs (using static field approach) are more suitable for distinguishing the SD fraction. However, it must be kept in mind that the coercivity of remanence may also be affected by magnetic mineral phases like Fe-sulphides, and caution should be taken when using the coercivity as a grain size indicator. A mixture of hard components such as greigite, hematite and goethite with soft magnetite in other sediments can compromise the use of remanence coercivity to some extent.

In brief, χ_{ARM}/χ , remanence coercivity spectra of ARM and delta ratios greater than 1.0 are sensitive parameters to determine the SD characteristics, but still cannot be used as sound indicators for bacterial origin.

6. Conclusions

1. The rock magnetic analyses of recent sediments of Lake Chiemsee strongly suggest the presence of fine-grained biogenic magnetite in the topmost 5 cm. This conjecture has been confirmed by TEM

observations of magnetic extracts, revealing intact cells and fossil magnetosomes of magnetite. Live magnetotactic bacteria have been detected with the Bacteriodrome.

2. The high concentration of live MTB at the top few centimetres and the dissolution of fine-grained magnetite with sediment depth are plausible explanations for the downcore variation of rock magnetic properties at the sampling sites. Because of the progressive dissolution of fine-grained magnetite with depth due to geochemical changes, the contribution of biogenic magnetite to the palaeomagnetic record of the lake sediment might diminish with burial time.
3. Low-temperature measurements on air-dried and freeze-dried sediment samples containing MTB yielded delta ratios (δ_{FC}/δ_{ZFC}) of 1.25 and 1.47, respectively, greater than 1.2 but lower than 2, and thus failed the Moskowitz test. Likely causes for the lower delta ratios are the presence of detrital magnetite, disrupted magnetosome chains, and possibly incipient low-temperature oxidation of the magnetosomes.
4. Measurements of acquisition and demagnetization spectra of ARMs and SIRMs, and values of χ_{ARM} are feasible alternative approaches for detecting SD magnetite in bulk sediments and assessing its contribution to the bulk magnetic properties.
5. Overall, rock magnetic methods are the most efficient tools for rapidly screening large quantities of sediments for bacterial magnetite. The complementary aids of TEM analyses are indispensable to unambiguously identify their bacterial origin.

Acknowledgements

We thank T. Frederichs for kind assistance with low-temperature measurements, U. Struck for help with the pore-water analyses and in sampling, C. Heunemann, R. Leonhardt and D. Krása for useful discussions. We are also pleased to acknowledge constructive reviews by B. Moskowitz and D. Faivre. YXP is grateful to the Alexander von Humboldt Stiftung (Germany) for granting a fellowship and supporting his stay in the LMU Munich. This work was supported by NSFC (grants 40325011 and 40221402).

References

- [1] R. Blakemore, Magnetotactic bacteria, *Science* 190 (1975) 377–379.
- [2] N. Petersen, T.v. Dobeneck, H. Vali, Fossil bacterial magnetite in deep sea sediments from the South Atlantic Ocean, *Nature* 320 (1986) 611–615.
- [3] J.F. Stolz, S.B.R. Chang, J.L. Kirschvink, Magnetotactic bacteria and single-domain magnetite in hemipelagic sediments, *Nature* 321 (1986) 611–849.
- [4] D.A. Bazylinski, R.B. Frankel, H.W. Jannasch, Anaerobic magnetite production by a marine, magnetotactic bacterium, *Nature* 334 (1988) 518–519.
- [5] J.W.E. Fassbinder, H. Stanjek, H. Vali, Occurrence of magnetic bacteria in soil, *Nature* 343 (1990) 161–163.
- [6] H. Petermann, U. Bleil, Detection of live magnetotactic bacteria in South Atlantic deep-sea sediments, *Earth Planet. Sci. Lett.* 117 (1993) 223–228.
- [7] I.F. Snowball, Bacteria magnetite and the magnetic properties of sediments in Swedish lake, *Earth Planet. Sci. Lett.* 126 (1994) 129–142.
- [8] J.A. Peck, J.W. King, Magnetofossils in the sediment of Lake Baikal, Siberia, *Earth Planet. Sci. Lett.* 140 (1996) 159–172.
- [9] S.B.R. Chang, J.L. Kirschvink, Magnetofossils, the magnetization of sediments, and the evolution of magnetite biomineralization, *Annu. Rev. Earth Planet. Sci.* 17 (1989) 169–195.
- [10] P.P. Hesse, Evidence for bacterial palaeo-ecological origin of mineral magnetic cycles in oxic and sub-oxic Tasman Sea sediments, *Mar. Geol.* 117 (1994) 1–17.
- [11] T. Yamazaki, H. Kawahata, Organic carbon flux controls the morphology of magnetofossils in marine sediments, *Geology* 26 (1998) 1064–1066.
- [12] I.F. Snowball, L. Zillén, P. Sandgren, Bacterial magnetite in Swedish varved lake-sediments: a potential bio-marker of environmental change, *Quat. Int.* 88 (2002) 13–19.
- [13] R. Egli, Characterization of individual rock magnetic components by analysis of remanence curves: 3. Bacterial magnetite and natural processes in lakes, *Phys. Chem. Earth* 29 (2004) 869–884.
- [14] Ø. Paasche, R. Løvlie, S.O. Dahl, J. Bakke, A. Nesje, Bacterial magnetite in lake sediments: late glacial to Holocene climate and sedimentary changes in northern Norway, *Earth Planet. Sci. Lett.* 223 (2004) 319–333.
- [15] K. Hilgenfeldt, Diagenetic dissolution of biogenic magnetite in surface sediments of the Benguela upwelling system, *Int. J. Earth Sci.* 88 (2000) 630–640.
- [16] N. Petersen, D.G. Weiss, H. Vali, Magnetic bacteria in lake sediments, in: Lowes, et al., (Eds.), *Geomagnetism and Paleomagnetism*, Kluwer Academic Publishers, 1989, pp. 231–241.
- [17] M. Hanzlik, M. Winklhofer, N. Petersen, Spatial arrangement of chains of magnetosomes in magnetotactic bacteria, *Earth Planet. Sci. Lett.* 145 (1996) 125–134.
- [18] B.M. Moskowitz, R.B. Frankel, D.A. Bazylinski, Rock magnetic criteria for the detection of biogenic magnetite, *Earth Planet. Sci. Lett.* 120 (1993) 283–300.
- [19] C. Heunemann, Gesteinsmagnetische und elektronenmikroskopische Untersuchungen an rezenten Seesedimenten, Diplomarbeit, Universität München, 1998.
- [20] M. Hanzlik, Elektronenmikroskopische und magnetomineralogische Untersuchungen an magnetotaktischen Bakterien des Chiemsees und bakteriellem Magnetit eisenreduzierender Bakterien, Dissertation am Institut für Allg. und Angew. Geophysik, Universität München, 1999, 152 pp.
- [21] S. Cisowski, Interacting vs. non-interacting single-domain behavior in natural and synthetic samples, *Phys. Earth Planet. Inter.* 26 (1981) 56–62.
- [22] H.P. Johnson, W. Lowrie, D.V. Kent, Stability of anhysteretic remanent magnetization in fine and coarser magnetite and maghemite particles, *Geophys. J. R. Astron. Soc.* 41 (1975) 1–10.
- [23] V.P. Shcherbakov, M. Winklhofer, M. Hanzlik, N. Petersen, Elastic stability of chains of magnetosomes in magnetotactic bacteria, *Eur. Biophys. J.* 26 (1997) 319–326.
- [24] K. Fabian, A. Kirchner, W. Williams, F. Heider, T. Leibl, A. Hubert, Three-dimensional micromagnetic calculations for magnetite using FFT, *Geophys. J. Int.* 124 (1996) 89–104.
- [25] D.C. Golden, D.W. Ming, C.S. Schwandt, H.V. Lauer, R.A. Socki, R.V. Morris, G.E. Lofgren, G.A. McKay, A simple inorganic process for formation of carbonates, magnetite, and sulphides in Martian meteorite ALH84001, *Am. Mineral.* 86 (2001) 370–375.
- [26] Y.X. Pan, R.X. Zhu, J.Y. Ping, Mineralogical alteration of siderite thermal-treated in air: moessbauer spectroscopy results, *Chin. Sci. Bull.* 44 (1999) 1712–1716.
- [27] H. Vali, J.L. Kirschvink, Magnetofossil dissolution in a palaeomagnetically unstable deep-sea sediment, *Nature* 339 (1989) 203–206.
- [28] B.M. Moskowitz, Biomineralization of magnetic minerals, *Rev. Geophys.* 33S1 (1995) 123–128.
- [29] D. Schüller, R.B. Frankel, Bacterial magnetosomes: microbiology, biomineralization and biotechnological applications, *Appl. Microbiol. Biotechnol.* 52 (1999) 464–473.
- [30] N. Otsuka, H. Sato, Observation of the Verwey transition in Fe_3O_4 by high-resolution electron microscopy, *J. Solid State Chem.* 61 (1986) 212–222.
- [31] R. Aragon, D. Buttrey, J.P. Shepherd, J.M. Honig, Influence of nonstoichiometry on the Verwey transition, *Phys. Rev., B* 31 (1985) 430–436.
- [32] B.P. Weiss, S.S. Kim, J.L. Kirschvink, R.E. Kopp, M. Sankaran, A. Kobayashi, A. Komeili, Ferromagnetic resonance and low-temperature magnetic test for biogenic magnetite, *Earth Planet. Sci. Lett.* 224 (2004) 73–89.
- [33] B. Carter-Stiglitz, B. Moskowitz, M. Jackson, More on the low-temperature magnetism of stable single domain magnetite: reversibility and non-stoichiometry, *Geophys. Res. Lett.* 31 (2004) doi:10.1029/2003GL019155.
- [34] P.W. Readman, W. O'Reilly, Magnetic properties of oxidized (cation-deficient) titanomagnetites, $(\text{Fe,Ti})_3\text{O}_4$, *J. Geomagn. Geoelectr.* 24 (1972) 69–90.
- [35] E. Senderov, A.U. Dogan, A. Navrotsky, Nonstoichiometry of magnetite–ulvospinel solid solutions quenched from 1300 °C, *Am. Mineral.* 78 (1993) 565–573.

- [36] F. Oldfield, Toward the discrimination of fine-grained ferrimagnets by magnetic measurements in lake and near-shore marine sediments, *J. Geophys. Res.* 99 (1994) 9045–9095.
- [37] F.D. Stacey, S.K. Banerjee, *The physical principles of rock magnetism*, Elsevier, Amsterdam, 1974, 195 pp.
- [38] B.M. Moskowitz, R.B. Frankel, P.J. Flanders, R.P. Blakemore, B.B. Schwartz, Magnetic properties of magnetotactic bacteria, *J. Magn. Magn. Mater.* 73 (1988) 273–288.
- [39] H.-U. Worm, H. Markert, Magnetic hysteresis properties of fine particles titanomagnetites precipitated in a silicate matrix, *Phys. Earth Planet. Inter.* 46 (1987) 84–92.
- [40] T. Pick, L. Tauxe, Characteristics of magnetite in submarine basaltic glass, *Geophys. J. Int.* 119 (1994) 116–128.
- [41] F. Heider, D.J. Dunlop, N. Sugiura, Magnetic properties of hydrothermally recrystallized magnetite crystals, *Science* 236 (1987) 1287–1290.
- [42] L. Tauxe, H.N. Bertram, C. Seberino, Physical interpretation of hysteresis loops: micromagnetic modelling of fine particle magnetite, *Geochem. Geophys. Geosyst.* (2002) doi:10.1029/2001GC000280.
- [43] S.B.R. Chang, J.L. Kirschvink, J.F. Stolz, Biogenic magnetite as a primary remanence carrier in limestone deposits, *Phys. Earth Planet. Inter.* 46 (1987) 289–303.